Performance optimization of a multi-channel transmit coil with significant coupling between elements

M. Kozlov[1], and R. Turner[1]

[1]Neurophysics, Max Planck Institute for Human Cognitive and Brain Sciences, Leipzig, Sachsen, Germany

Purpose: Most published studies of multi-channel transmit coils report only the radiation losses, single element reflection ($\mathbf{S_{xx}}$) and power absorbed by phantoms or human body models. However, at higher frequency the power reflected by the entire coil ($\mathbf{P_{ref\_coil}}$) as well as the surface and volume losses in coil elements become important for understanding the coil performance. Our goal was to investigate all losses of a commercially available multi-channel coil with significant coupling ($\mathbf{S_{xy}}\approx 7$ dB) between neighboring elements, and the influence of coil tuning strategy on coil performance.

Method: We employed co-simulation of the RF circuit and 3-D EM fields. Agilent ADS was used as the RF circuit tool, and CST and HFSS were used as 3-D EM tools. This approach significantly speeds up the analysis of a multi-channel transmit coil, since one 3-D EM simulation is sufficient for investigation of the coil behavior with different tunings. The coil 3-D EM model includes all construction details for the resonance elements, simulated with realistic dimensions and material electrical properties. For tuning at the MRI resonance frequency of 297.2 MHz ($\mathbf{f_{res}}$), a Siemens water-based phantom was placed inside the coil, and the in-vivo coil performance was evaluated using the Ansoft human body and HUGO models (both with different scaling factors: 1, 09, 0.8) and also all models of the "Virtual Family" data set. The number of mesh cells was increased in the CST and HFSS simulations until there was no significant difference between the simulated and experimental trim capacitor values. For the Siemens phantom as load, this condition was achieved using a 1 mm isotropic mesh size, with a total of 57.2 million mesh vertices for CST and 2 million tetrahedra for HFSS. In a bench experiment using the actual rf coil, the resonance frequency of the magnetic field for each element ($\mathbf{f_{elem}}$) was then measured, using a network analyzer connected to the coil input and a small single loop coil placed in the geometrical centre of the element (S_{21} measurement setup). The frequency at which $\mathbf{S_{xx}}$ approaches its minimum ($\mathbf{f_{min\_Sxx}}$) was measured by direct connection to the element input with simultaneous termination of other elements by 50 Ohm loads. In further work, MRI measurements of $\mathbf{B_1+}$ using this coil were performed on a Siemens 7T scanner.

Results and Discussion: Different tuning conditions were investigated. These were: a) vendor provided tuning – all $\mathbf{f_{min\_Sxx} = f_{res}}$; b) all $\mathbf{f_{elem} = f_{res}}$; c) $\mathbf{P_{ref\_coil}}$ approaches its minimum at $\mathbf{f_{res}}$; and some alternative tuning arrangements. RF circuit simulation data (**S** parameter matrix, element-specific Q factors, $\mathbf{f_{elem}}$'s) and 3-D EM simulation data ($\mathbf{B_1+}$ profile) were both found to be almost equal to the corresponding measured data for the rf coil, using Siemens water- and oil-based phantoms inside the coil. This was true both for vendor-provided and a previously tested alternative tuning. By coil re-tuning it is possible to reduce $\mathbf{P_{ref\_coil}}$ at $\mathbf{f_{res}}$ from more than 43% of transmitted power to less than 11%, with simultaneous increases of as much as 33% for the average $\mathbf{B_1+}$ within the brain volume (Table 1). This numerical prediction was demonstrated by experimental $\mathbf{B_1+}$ mapping of a re-tuned coil that quantitatively confirmed this increase in $\mathbf{B_1+}$. The reason for this is as follows: for any tuning stage, $\mathbf{f_{elem}}$ differs from $\mathbf{f_{min\_Sxx}}$ by several MHz, for the same element. With every tuning arrangement that equalizes $\mathbf{f_{min\_Sxx}}$, the $\mathbf{f_{elem}}$'s consequently differ by several MHz from each other, and from this $\mathbf{f_{min\_Sxx}}$. The same is true for the opposite case (Fig.1). As a result, requiring all $\mathbf{f_{elem}}$ to be equal to $\mathbf{f_{res}}$ offers much better performance than tuning all $\mathbf{f_{min\_Sxx}}$ to be equal to $\mathbf{f_{res}}$. Further investigations confirmed that the coil's performance (i.c. magnetic field) approaches a maximum when $\mathbf{P_{ref\_coil}}$ is minimal (Table 1). Coil tuning is not trivial in this case, since for a multi-channel coil with significant coupling between elements, $\mathbf{P_{ref\_coil}}$ depends not only on the $\mathbf{S_{xy}}$ magnitudes, which vary slightly for different tunings, but also on the phase distribution of both $\mathbf{S_{xy}}$ and the power delivered to each coil element. However, without considerable performance degradation $\mathbf{f_{elem}}$ can vary in about +/- 0.5 MHz tuning range of around the frequency for optimal coil performance because loaded coil element **Q**-factor is rather small (about 30). Use of the trim capacitors available to tune each $\mathbf{f_{elem}}$ allows slight adjustment of the $\mathbf{B_1+}$ profile in the transverse plane (Fig. 2). But for all configurations there are intrinsic differences in current magnitude within the coil elements at $\mathbf{f_{res}}$ (Fig. 1) that cannot be explained only by geometric factors. For all tuning cases and loads, radiation losses were not the major losses (excluding losses due to coil loading). In fact, these were less than 65% of the coil element resistive losses. Most of these resistive losses arise from the fact that rf current flows only on the edges of the copper strips. For the same coil loading, the resistive, dielectric and radiation losses are basically proportional to the current through the coil elements. Using simulations with different human models, the array coil tuning can be adjusted to provide the best performance for a given head mass and shape distribution.

The reflected power $\mathbf{P_{ref\_coil}}$ is independent of whether the rf coil is used as a multi-channel transmit array or as a single channel transmitter, with a power splitter to distribute voltage with equal amplitude to each element, as long as the power splitter does not transform the impedance. If the power splitter is designed to absorb most of the reflected power $\mathbf{P_{ref\_coil}}$, SAR safety monitoring becomes more complex, because it is difficult to monitor the power absorbed by the coil alone.

Conclusion: The $\mathbf{S_{xx}}$ data do not reveal the important frequency splitting that occurs in a multi-channel coil with significant coupling between elements. Performance of such a coil would be considerably improved if the coil can be tuned to minimize $\mathbf{P_{ref\_coil}}$ at $\mathbf{f_{res}}$, which is not possible using simple measurement of $\mathbf{S_{xx}}$. If the capacitance values obtained by simulation and actual trim tuning procedures are found to be equal, the close agreement between simulated and measured data is only limited by uncertainties in the geometrical and electrical properties provided by manufacturers for the MRI scanner hardware and the rf coil.

Load	Siemens phantom			Head scaling factor =1			Head scaling factor =0.9			Head scaling factor =0.8		
Tuning condition	$\mathbf{f_{min\_Sxx}} = \mathbf{f_{res}}$	$\mathbf{f_{elem}} = \mathbf{f_{res}}$	$\mathbf{P_{ref\_coil}}$ is min at $\mathbf{f_{res}}$	$\mathbf{f_{min\_Sxx}} = \mathbf{f_{res}}$	$\mathbf{f_{elem}} = \mathbf{f_{res}}$	$\mathbf{P_{ref\_coil}}$ is min at $\mathbf{f_{res}}$	$\mathbf{f_{min\_Sxx}} = \mathbf{f_{res}}$	$\mathbf{f_{elem}} = \mathbf{f_{res}}$	$\mathbf{P_{ref\_coil}}$ is min at $\mathbf{f_{res}}$	$\mathbf{f_{min\_Sxx}} = \mathbf{f_{res}}$	$\mathbf{f_{elem}} = \mathbf{f_{res}}$	$\mathbf{P_{ref\_coil}}$ is min at $\mathbf{f_{res}}$
Power accepted by entire coil, [W]	4.26	6.66	7.13	4.47	7.33	7.57	4.54	6.97	7.41	4.82	6.73	7.31
Radiated power, [W]	0.73	1.14	1.20	0.62	1.02	1.06	0.86	1.32	1.40	1.06	1.48	1.61
Power accepted by load, [W]	2.13	3.36	3.62	2.68	4.47	4.59	2.38	3.69	3.92	2.37	3.35	3.65
Power accepted by dielectrics, [W]	0.21	0.30	0.31	0.17	0.26	0.27	0.19	0.27	0.29	0.21	0.26	0.29
Power accepted by conductors, [W]	1.19	1.86	2.00	1.00	1.58	1.65	1.11	1.69	1.80	1.18	1.64	1.76
B1+ average over brain [A/m]				0.55	0.70	0.73	0.68	0.84	0.88	0.76	0.91	0.96

Table 1.

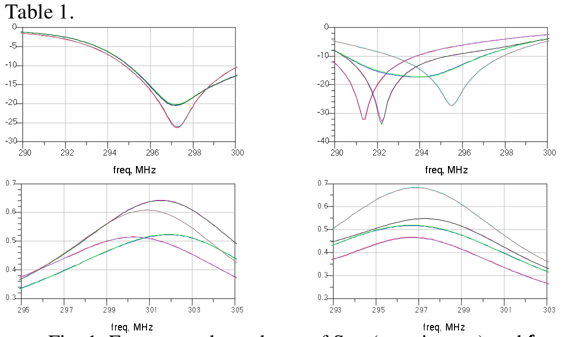

Fig. 1. Frequency dependence of Sxx (top pictures) and $\mathbf{f_{elem}}$. Vendor provided tuning (left row), all $\mathbf{f_{elem}} = \mathbf{f_{res}}$ (right row).

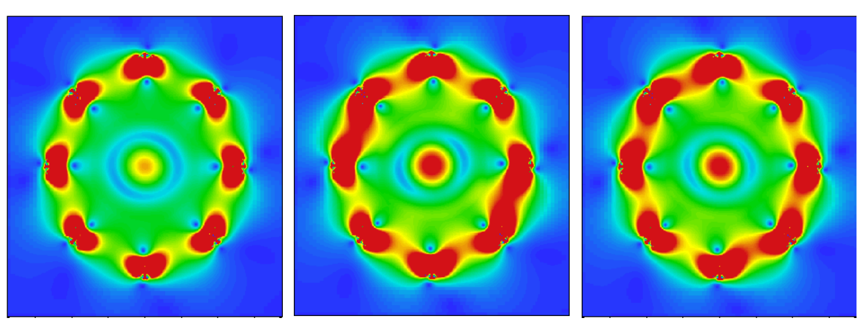

Fig. 2. B1+ transverse profile of Siemens phantom for vendor provided tuning (left), $\mathbf{f_{elem}} = \mathbf{f_{res}}$ (center), $\mathbf{P_{ref\_coil}}$ is min at $\mathbf{f_{res}}$ (right).